

Dissolution state of cellulose in aqueous systems. 1. Alkaline solvents

Luis Alves · Bruno Medronho ·
Filipe E. Antunes · Daniel Topgaard ·
Björn Lindman

Received: 8 October 2015 / Accepted: 30 October 2015 / Published online: 4 November 2015
© Springer Science+Business Media Dordrecht 2015

Abstract The understanding of the state of dissolution of cellulose in a certain solvent is a critical step forward in the development of new efficient solvent systems for cellulose. Nevertheless, obtaining such information is not trivial. Recently, polarization transfer solid-state NMR (PTssNMR) was shown to be a very promising technique regarding an efficient and robust characterization of the solution state of cellulose. In the present study, combining PTssNMR, microscopic techniques and X-ray diffraction, a set of alkaline aqueous systems are investigated. The addition of specific additives, such as urea or thiourea, to

aqueous NaOH based systems as well as the use of an amphiphilic organic cation, is found to have pronounced effects on the dissolution efficiency of cellulose. Additionally, the characteristics of the regenerated material are strongly dependent on the dissolution system; typically less crystalline materials, presenting smoother morphologies, are obtained when amphiphilic solvents or additives are used.

Keywords Amphiphilicity · Chain packing · PTssNMR · NaOH · TBAH

L. Alves (✉) · F. E. Antunes
Department of Chemistry, University of Coimbra,
3004-535 Coimbra, Portugal
e-mail: luisalves@ci.uc.pt

B. Medronho
Faculty of Sciences and Technology (MEDITBIO),
University of Algarve, Campus de Gambelas, Ed. 8,
8005-139 Faro, Portugal

D. Topgaard
Division of Physical Chemistry, Department of
Chemistry, Center for Chemistry and Chemical
Engineering, Lund University, 221 00 Lund, Sweden

B. Lindman
Materials Science and Engineering, Nanyang
Technological University, Singapore 639798, Singapore

B. Lindman
FSCN, Mid Sweden University, 851 70 Sundsvall,
Sweden

Introduction

Cellulose is very recalcitrant to dissolution in most of the common solvent systems; water and most organic solvents are among the large number that fails in this respect. Cellulose insolubility is typically attributed to an extended intra- and inter-molecular network of hydrogen bonds (Kamide et al. 1985; Klemm et al. 2005; Sen et al. 2013) but recent discussions also highlight the role of the hydrophobic interactions on the insolubility of cellulose (Kalashnikova et al. 2012; Lindman et al. 2010; Medronho and Lindman 2014; Medronho et al. 2012; Yamane et al. 2006). Thus it is suggested that an efficient dissolution medium for an amphiphilic molecule, such as cellulose, should also have an amphiphilic character, or intermediate polarity, in order to reduce/eliminate the existing hydrophobic interactions. Not only the mechanisms governing

cellulose dissolution are still under debate but there are also a lack of facile and accurate techniques capable of providing a clear understanding on the level of cellulose dissolution and its molecular organization. How well dissolved cellulose is and how it organizes in solution are key issues often neglected in the literature. Typically, a clear optical micrograph, with no perceptible visible insoluble material is used to decide if cellulose is dissolved or not. However, this two-option rule does not always hold; intermediate stages between swelling and complete solubility exist and in cellulose solutions this is striking. While such a simplistic approach is obviously useful, for an initial solvent screening and characterization, one should be aware that, in the majority of the applications, understanding how cellulose behaves in solution, and how it is organized, may be very important to rationalize the properties of a given regenerated material. Several experimental techniques can be applied to study cellulose, but most of them are mainly suitable to either the starting or the final materials, leaving the solution state without a deep thorough characterization. Examples of traditional characterization methods widely used in the cellulose field are infrared spectroscopy (O'Connor et al. 1958; Široký et al. 2010), wide angle X-ray scattering (used in powders and fibers) (Garvey et al. 2005; Langan et al. 2001), electronic microscopy (transmission and scanning) (Hao et al. 2015; Luo et al. 2012), and solid-state nuclear magnetic resonance (NMR) (Kamide et al. 1985; VanderHart and Atalla 1984). Among these, and despite all the complicated experimental details associated, cryo-TEM, small angle X-ray scattering (Rein et al. 2014) and high resolution solid-state NMR (Nehls et al. 1994) are commonly used to study cellulose in solution.

Recently, Topgaard et al. suggested an experimental approach based on a newly developed NMR methodology (Nowacka et al. 2010). This technique combines features of both high resolution and solid-state NMR, thus enabling studies of all the constituent phases in complex materials with solid, liquid and liquid-crystalline domains. The method has been applied to systems containing amphiphilic molecules in different physical states as hydrated surfactants (Nowacka et al. 2010, 2013), biomembranes (Nowacka et al. 2012), lipid-amyloid fibril aggregates (Hellstrand et al. 2013), and stratum corneum (Björklund et al. 2013). Recently, polarization transfer solid-state NMR (PTssNMR) has

also been shown to successfully provide molecular-level information on the dissolved and insoluble fractions of cellulose in an aqueous dissolving medium (Gustavsson et al. 2014). The PTssNMR technique takes advantage of the ^{13}C chemical shifts, that provide information on the molecular structure, conformation, and chain packing, but also on the molecular dynamics via the signal intensities obtained with the polarization transfer schemes CP (cross polarization) (Pines et al. 1972) and INEPT (insensitive nuclei enhanced by polarization transfer) (Morris and Freeman 1979). The CP and INEPT techniques are traditionally used to boost the signals for solids and liquids, respectively, in comparison to the ^{13}C direct polarization (DP).

Striking differences in cellulose dissolution between two alkaline solvents have previously been reported, highlighting the fundamental differences between a small inorganic cation of high charge density and a large organic cation with amphiphilic character (Alves et al. 2015; Gustavsson et al. 2014). Here we extend the previous work using a larger number of alkaline systems and additives to get information on the dissolution efficiency by means of light and electron microscopy, X-ray and PTssNMR, where the latter technique is given special attention.

Materials and methods

Materials

Microcrystalline cellulose Avicel PH-101, with an average particle size of 50 μm and degree of polymerization of ca. 260, zinc oxide (>99 % purity), urea (99.5 % purity), thiourea (>99 % purity), alkyl-polyglucoside (APG) 50 % solution, tetrabutylphosphonium hydroxide (TBPH) (40 % solution in water) and tetrabutylammonium hydroxide (TBAH) of chromatographic grade (as a 40 wt% solution in water) were acquired from Sigma Aldrich. NaOH pellets (>98 % purity) was obtained from Fluka. All chemicals were used as received.

Methods

Sample preparation

Cellulose dissolution was achieved following the adapted standard procedures in literature (Hao et al.

2015; Ioelovich 2012; Lu and Shen 2011). Briefly, the alkali based systems were prepared by the addition of 10 wt% of cellulose (and additives, when used) in a 8 wt% NaOH/H₂O solution, which was then allowed to freeze at $-20\text{ }^{\circ}\text{C}$ for 24 h. This was followed by thawing the solid frozen mass at room temperature with simultaneous vigorous mixing. On the other hand, for the TBAH and TBPH based solvents, the dissolution procedure was simply the mixture of 10 wt% of cellulose with a 40 wt% TBAH or TBPH aqueous solution at room temperature for 30 min.

PTssNMR

NMR experiments were performed at the ¹H and ¹³C Larmor frequencies of 500 and 125 MHz, respectively, on a Bruker AVII-500 spectrometer, with a 4 mm ¹³C/³¹P/¹H E-free probe (Bruker, Germany). The ¹³C spectra were acquired under 88 kHz two-phase pulse modulation (TPPM) decoupling, using 20 ms acquisition time with 300 ppm spectral width, and a 80 kHz nutation frequency for the 90° and 180° pulses. The spectra were acquired using 4 mm HR-MAS rotors (Bruker, Germany), specifically designed for retaining liquids during magic angle spinning (MAS), at a spinning frequency of 5 kHz. CP was performed with $\tau_{\text{CP}} = 1\text{ ms}$, 80 kHz ¹³C nutation frequency, linearly ramped from 72 to 88 kHz ¹H nutation frequency. The time delays of $\tau = 1.8\text{ ms}$ and $\tau' = 1.2\text{ ms}$ were used for refocused INEPT. For each spectrum 3072 transients were accumulated, with 5 s recycle delay, giving a total measurement time of 12.5 h per sample. The ¹³C spectra were externally referenced to alpha-glycine at 43.67 ppm (α carbon). The spectra were collected at 25 °C. Processing was performed using a Fourier transform with 100 Hz line broadening, zero-filling from 755 to 8192 complex points, automatically phase and baseline corrected, using customized Matlab scripts based on matNMR.

Scanning electron microscopy

A high resolution (Schottky) Scanning Electron Microscope, equipped with the analytical systems X-ray microanalysis (EDS) and backscattered electron diffraction pattern analysis (EBSD), was used to observe the solution state of the cellulose dopes (model Quanta 400FEG ESEM/EDAX Genesis X4M). Generally, 50 μL of solution was dropped

onto a clean glass lamella followed by drying for 24 h in a kiln and then sputtered with an approximately 6 nm thin Au/Pd film by cathodic pulverization using a SPI Module Sputter Coater before SEM analysis, during 90 s with a current of 15 mA. The starting and regenerated materials (powders) were deposited directly over the carbon tape on the support and sputtered following the procedure previously described. The accelerating voltage ranged from 5 to 15 kV.

X-ray diffraction

The X-ray diffraction (XRD) experiments were performed on a Siemens D5000 X-ray diffractometer, capable of identifying crystalline phases down to 3 % of the bulk. A CuK _{α 1} radiation source with $\lambda = 1.54056\text{ \AA}$, focused by a primary Ge crystal monochromator, was used. The detector is a standard scintillation counter. The Cu tube runs at 40 mA and 40 kV. The cooling is supplied by an internal water-filled recirculation chilling system, running at approximately 16 °C with a flow rate of 4–4.5 L/min. The slit arrangement is a 2 mm pre-sample slit, 2 mm post sample slit and a 0.2 mm detector slit. The freeze-dried cellulose powders were placed in a proper support and analyzed.

Polarized light microscopy

A Linkam LTS 120 microscope equipped with a Q imaging (Qicam) Fast 1394 camera was used to observe the cellulose dissolution in both NaOH and TBAH solvents. Samples were kept between cover slips and illuminated with linearly polarized light and analyzed through a crossed polarizer. Images were captured and analyzed using Qcapture software.

Results and discussion

In a previous work striking differences in the cellulose dissolution performance between solvents containing small inorganic cations and amphiphilic cations were found and suggested support for the critical role of hydrophobic interactions between cellulose molecules (Alves et al. 2015; Gustavsson et al. 2014).

Figure 1 shows the polarized light micrographs of cellulose dissolved in different alkaline aqueous

media. It is possible to observe that an alkaline solvent doped with thiourea (Fig. 1c) is more efficient than its counterpart without the additive since in the latter case small disks and insoluble material are still visible (Fig. 1b). The same enhancement in dissolution is found for other additives such as urea or an alkyl polyglycoside surfactant. Likewise, the micrograph of the TBAH system shows no signs of undissolved material (Fig. 1d) while, as expected, no dissolution is achieved in pure water (Fig. 1a). These observations are in line with our previous work and indicate that the dissolution of cellulose is facilitated by solvents with amphiphilic properties, such as TBAH or NaOH doped with specific additives.

In Fig. 2, SEM micrographs are shown for microcrystalline cellulose dissolved in the different alkaline systems. Each specimen was prepared by depositing a small droplet of the cellulose solution onto a glass lamella followed by drying the solvent. Quite different morphologies are identified.

For the cellulose sample dissolved in aqueous NaOH it is possible to observe undissolved crystallites with an average length of a few microns. It is important to note that the energy dispersive

spectroscopy (EDS) spectra indicates that such needle-like crystallites are indeed cellulose and not NaOH or other dry inorganic compounds (data not shown) in agreement with previous reported data (Alves et al. 2015). On the other hand, the sample containing an additive with intermediate polarity (thiourea) shows a continuous-like “melted” film, without any undissolved crystallites (Fig. 2c). A similar result was obtained for the TBAH sample, where a “continuous wrinkled” flexible film is observed, also without any visible undissolved crystallites. The absence of crystals in the latter samples demonstrates the enhanced dissolution efficiency of a solvent with amphiphilic properties.

The majority of the advanced microscopy techniques applied in the cellulose field, such as scanning or transmission electron microscopy, requires samples in the dry state and complicated protocols. As alluded above, although these methods might be useful for the characterization of the morphology and texture of the material, they lack in a reliable description of the molecular state and organization of the cellulose molecules in solution since, in most cases, the solvent is absent. The PTssNMR method not only is of

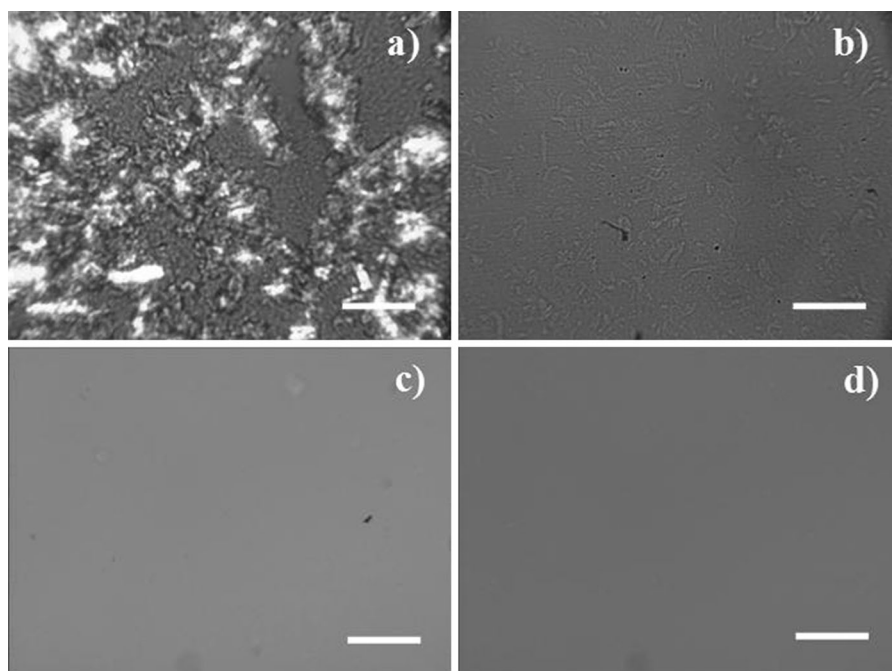


Fig. 1 Polarized light micrographs of 5.0 wt% microcrystalline cellulose dispersed in **a** water, **b** dissolved in 8.0 wt% NaOH aqueous solution, **c** in 40.0 wt% TBAH aqueous and **d** in 8.0 wt% NaOH/12.0 wt% thiourea aqueous. The scale bar 100 μm

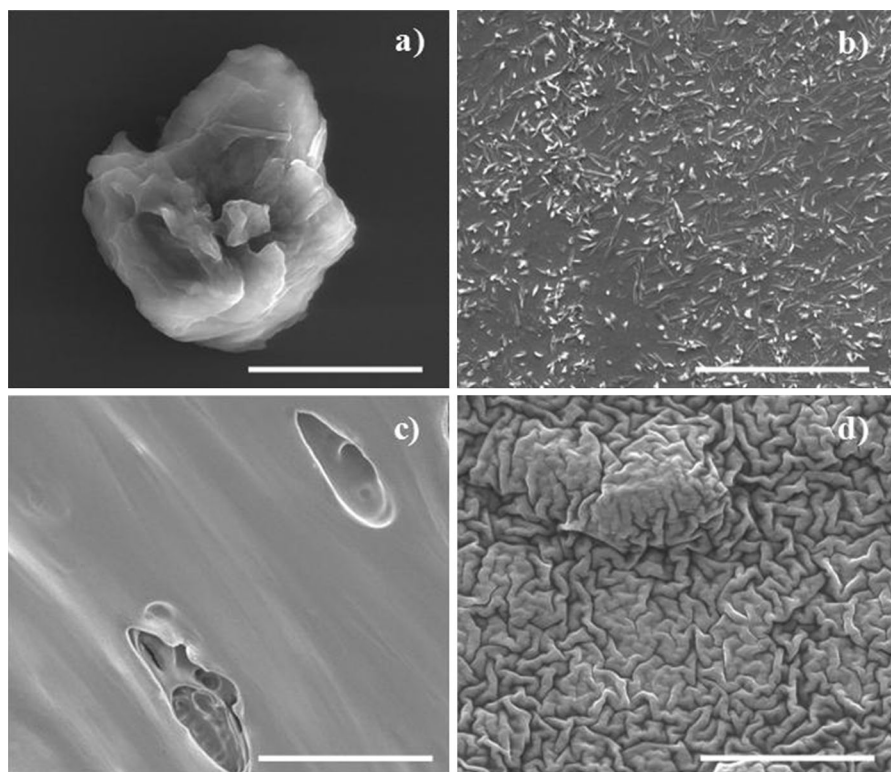


Fig. 2 Scanning electron micrographs of dried samples of microcrystalline cellulose after being **a** dispersed in water, **b** dissolved in aqueous NaOH, **c** dissolved in aqueous NaOH/thiourea and **d** dissolved in aqueous TBAH. The scale bar 10 μm

reasonable facile application but also provides robust molecular information as described in the introduction. In Fig. 3 the PTssNMR spectra of microcrystalline cellulose (MCC) dissolved in aqueous NaOH and TBAH, are depicted together with the spectrum of the native MCC.

The main information (i.e. chemical shifts and type of crystalline polymorph) extracted from Fig. 3 is summarized in Table 1. Note that the information for the TBPH system is also present in Table 1.

The starting material gives intense CP peaks while no INEPT signal is detected (top spectra). This is expected for a material in a solid state as the native MCC powder. The observed CP chemical shifts are typical for a cellulose I crystalline organization (Porro et al. 2007) and the chemical shift values are in good agreement with literature (Kamide et al. 1985). The side peaks for the carbons C_4 and C_6 , at ca. 85 and 62 ppm, respectively, can be attributed to the residual amorphous fraction of cellulose present in the dried MCC (Kunze and Fink 2005). On the other hand, the

MCC sample dissolved in aqueous TBAH gives both CP and INEPT signals. However, the weak CP signal indicates a good level of dissolution. It is important to note that the huge signal from the TBA^+ carbons make rather small the INEPT signal for cellulose and therefore more susceptible to noise. Similar results were obtained for the TBPH solvent with no significant differences from the TBAH system. Alternative procedures are capable of reducing these huge solvent peaks, such as solvent suppression techniques, selective excitation (Zumbulyadis 1983) or methods based on T1-differences. These will be considered in future. The measured chemical shifts and the similarities between the CP spectra of the starting material (top spectra) and CP spectrum of MCC in aqueous TBAH (middle spectra), reveal that the undissolved solid fraction of MCC has a cellulose I crystalline organization. The INEPT spectrum presents a large peak, attributed to the TBA^+ carbons and some other small peaks (indicated with arrows) which, most likely, are breakdown products of TBAH (Gustavsson et al.

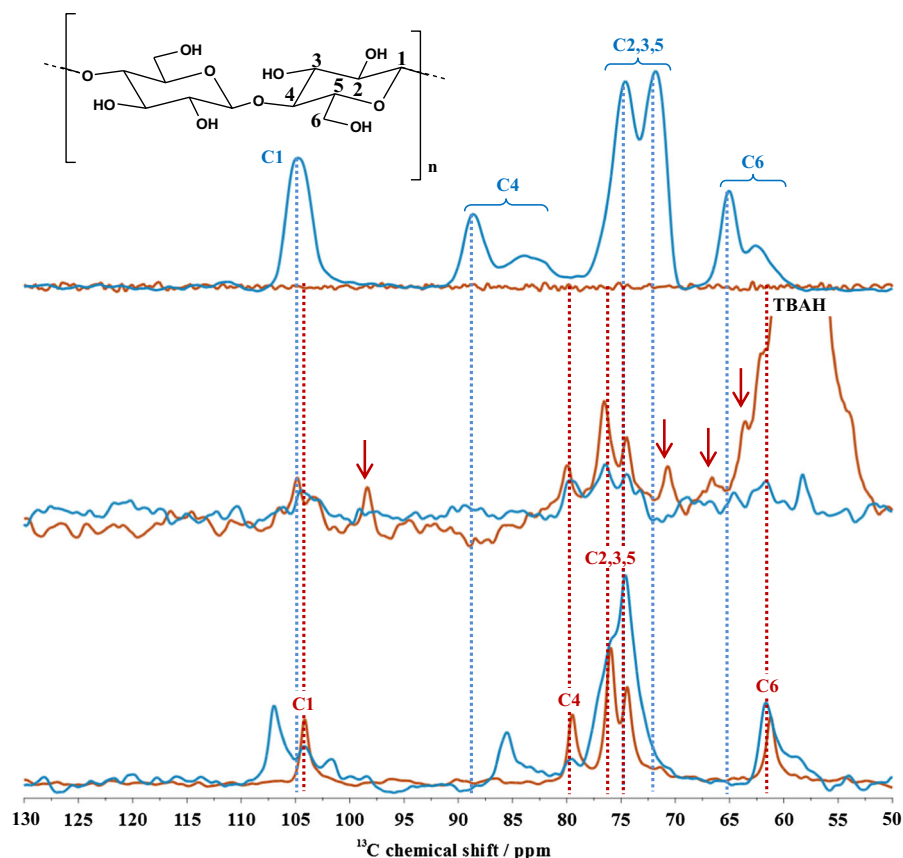


Fig. 3 PTssNMR data for microcrystalline cellulose in the initial dry state (*top*), as well as dissolved in aqueous TBAH (*middle*) and NaOH solution (*bottom*). The CP and INEPT spectra are shown in *blue* and *red*, respectively. The assignments of the solid (*blue*) and dissolved (*red*) cellulose peaks refer to the carbon atom numbering in the structural formula. The *blue* and *red* dashed lines literature data for cellulose I in wood pulp fibers (Kamide et al. 1985) and dissolved cellulose (Kamida et al.

1984), respectively. The labels TBAH point out the truncated peaks from the TBA⁺ ions, while the *arrows* TBA⁺ decomposition products. The data was acquired at 25 °C and 125 MHz ¹³C Larmor frequency with 5 kHz MAS and 88 kHz TPPM ¹H decoupling. The spectra are zoomed-in on the 50–130 ppm spectral region relevant for cellulose and, independently for each sample, magnified to facilitate observation of the cellulose resonance lines. (Color figure online)

2014). The INEPT peaks assigned to the dissolved cellulose are in very good agreement with the reported values in literature [i.e. 104.7 (C₁), 79.9 (C₄), 76.4/75.0 (C_{2,3,5}), and 61.9 (C₆) ppm] for ultra-centrifuged samples of cellulose dissolved in 10 wt% NaOH/D₂O (Kamida et al. 1984). According to theoretical calculations (Gustavsson et al. 2014), the presence of INEPT peaks for cellulose implies that the C–H bonds reorient on a timescale faster than 100 ns, which in turn is a strong indication that the “liquid fraction” of the cellulose solution is molecularly dissolved and thus does not represent cellulose aggregates.

The MCC sample dissolved in an aqueous NaOH solution gives both CP and INEPT signals (bottom

spectra). While the INEPT peaks present similar chemical shifts to the ones assigned to the dissolved fraction of cellulose in the TBAH system, the CP spectrum is significantly different; a comparison with the chemical shifts found in literature, [e.g. 106.9/104.2 (C₁), 85.5/83.0 (C₄) and 61.3 (C₆)] suggests that cellulose is organized as the so called “Na-cellulose Q”, which is a highly swelled form of cellulose first identified by Sobue et al. (Porro et al. 2007). This swelled state of cellulose is also characterized by a low order state, that can be deduced from the chemical shifts for C₄, (85.52 ppm), and C₆ (61.65 ppm) (Kunze and Fink 2005). Additionally, the NaOH sample presents a well defined CP spectrum (good

Table 1 ^{13}C chemical shifts of the dissolved and solid fractions of microcrystalline cellulose in the alkaline NaOH, TBAH and TBPH solvents

Sample	Fraction	Chemical shift/ppm ^a				Polymorph
		C ₁	C ₄	C _{2,3,5}	C ₆	
Dry	Solid	104.8	88.7	74.6, 71.8	65.1	Cellulose I
TBAH	Solid	104.5	89.4	76.4, 74.5	64.6	Cellulose I
	Dissolved	104.9	80.0	76.6, 74.5	61.8	
TBPH	Solid	104.8	88.9	76.0, 74.2	65.8	Cellulose I
	Dissolved	104.7	79.4	76.5, 74.3	62.3	
NaOH	Solid	107.0, 104.2, 101.7	85.5	74.6	61.7	Na-Cell. Q ^b
	Dissolved	104.2	79.5	76.0, 74.4	61.2	

^a Chemical shifts in ppm. The data were referenced using α -glycine as external standard at 43.67 ppm (α carbon). The precision is limited to ± 0.2 ppm by the acquisition time

^b Na-Cellulose Q is a highly swelled form of cellulose identified by Sobue et al. (Porro et al. 2007)

signal-to-noise ratio), which is indicative of a significant amount of undissolved material in solution, in contrast to the CP spectrum obtained for the TBAH sample, where the signal-to-noise ratio is considerably poorer.

The addition of specific additives with adequate polarity to the NaOH based solvent system can improve the dissolution of cellulose. In the literature, the use of urea (Kunze and Fink 2005; Luo and Zhang 2013), thiourea (Zhang et al. 2013), ZnO (Kihlman et al. 2013) and polyethylene glycol (PEG) (Yan and Gao 2008) has been highlighted. In Fig. 4, the CP and the INEPT spectra for MCC dissolved in NaOH/thiourea aqueous solution are depicted and, in Table 2 the polymorph type of the solid fraction and main chemical shift are summarized also for other NaOH systems doped with different additives.

As observed for the NaOH aqueous solvent, clear CP and INEPT signals are also detected for the cellulose dissolved in the NaOH/thiourea system thus indicating that dissolution is not complete. However, the ratio between the CP and INEPT peaks is different. Even if neither CP nor INEPT are truly quantitative, the relation between the peaks intensity is indicative of the undissolved/dissolved relation in solution. For the NaOH system the CP peaks are more intense than the INEPT peaks while this relation is inverted for NaOH/thiourea system. This suggests that the additive improves the dissolution efficiency as manifested by the enhancement in the INEPT signal. The chemical shifts obtained for the solid fraction of cellulose (CP

signal) in the NaOH/thiourea system, [104.7 (C₁), 86.4 (C₄), 76.2/75.3 (C_{2,3,5}) and 61.6 (C₆) ppm], can be assigned to a Na-cellulose II structure, with an anti-parallel arrangement of the cellulose molecules in the crystal, which is in good agreement with the literature (Kunze and Fink 2005).

The parallel arrangement found in the original MCC sample and also in nature (i.e. cellulose I), is not the most stable structure for a cellulose crystal; when dissolved and recrystallized, cellulose chains tend to adopt the cellulose II type crystal (Mittal et al. 2011). It has been postulated that the transition from a cellulose I to a cellulose II organization requires only a translational movement of cellulose molecules (Takai and Colvin 1978). Nevertheless, this is an intriguing process, and still not understood in detail.

It is worth noting that the INEPT spectra of cellulose dissolved in the NaOH/additives solvents present a slight downfield shift with an average value of ca. 0.4 ppm. This might be explained by an additive-cellulose interaction, which not only facilitates dissolution but is also expected to influence the carbon chemical shifts of cellulose (Wernersson et al. 2015). Recent studies tend to support this observation regarding a preferential additive-cellulose interaction. For instance, Bergensträhle-Wohlert et al. (2012), combining MD simulations and solid-state NMR on cellulose in water and in aqueous urea solutions, found that the local concentration of urea is significantly enhanced at the cellulose/solution interface. In another related study, Xiong et al. (2014) conclude that the

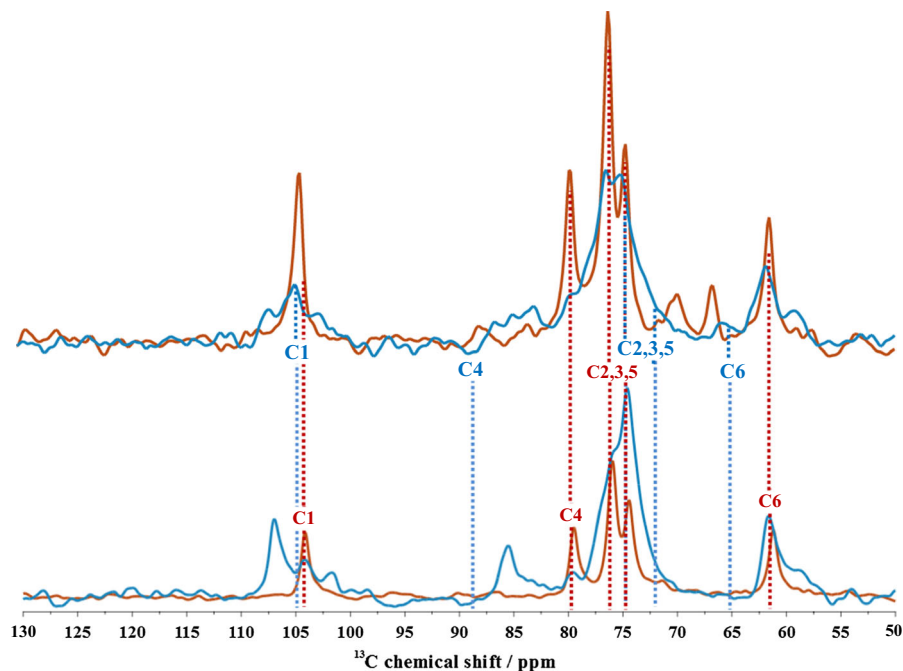


Fig. 4 CP (blue line) and INEPT (red line) spectra for 10 wt% microcrystalline cellulose dissolved in aqueous 8 % NaOH/12 % thiourea (top) and in aqueous 8 % NaOH (bottom). The data was acquired at 25 °C and 125 MHz ^{13}C Larmor frequency with 5 kHz MAS and 88 kHz TPPM ^1H decoupling. The spectra are expanded on the 50–130 ppm spectral region relevant for cellulose, and, independently for each sample, vertically

magnified to facilitate observation of the cellulose resonance lines. The blue and red dashed lines represent literature data for cellulose I in wood pulp fibers (Kamide et al. 1985) and dissolved cellulose (Kamida et al. 1984), respectively. The carbon atom numbering is according to the structural formula presented in Fig. 3. (Color figure online)

Table 2 ^{13}C chemical shifts of the dissolved and solid fractions of MCC in NaOH doped with different additives

Sample	Fraction	Chemical shift ^a				Polymorph
		C ₁	C ₄	C _{2,3,5}	C ₆	
NaOH	Solid	107.0, 104.2, 101.7	85.5	74.6	61.7	Na-Cell. Q ^b
	Dissolved	104.2	79.5	76.0, 74.4	61.2	
NaOH/ZnO	Solid	107.1, 104.9	85.7	76.1, 74.8	61.8	Na-Cell. Q ^b
	Dissolved	104.3	79.7	76.3, 74.8	61.5	
NaOH/Urea	Solid	103.8, 102.6	84.6	75.7	59.8	Amorphous
	Dissolved	104.6	80.0	75.8	61.3	
NaOH/Thio.	Solid	104.7	86.4	76.2, 75.3	61.6	Na-Cell. II
	Dissolved	104.3	79.6	76.1, 74.6	61.5	
NaOH/APG	Solid	106.8	86.0	75.3	61.7	Na-Cell. I
	Dissolved	104.8	79.7	76.5, 73.9	61.9	

^a Chemical shifts in ppm. The data were referenced using α -glycine as external standard at 43.67 ppm (α carbon). The precision is limited to ± 0.2 ppm by the acquisition time

^b Na-cellulose Q is a highly swelled form of cellulose identified by Sobue et al. (Porro et al. 2007)

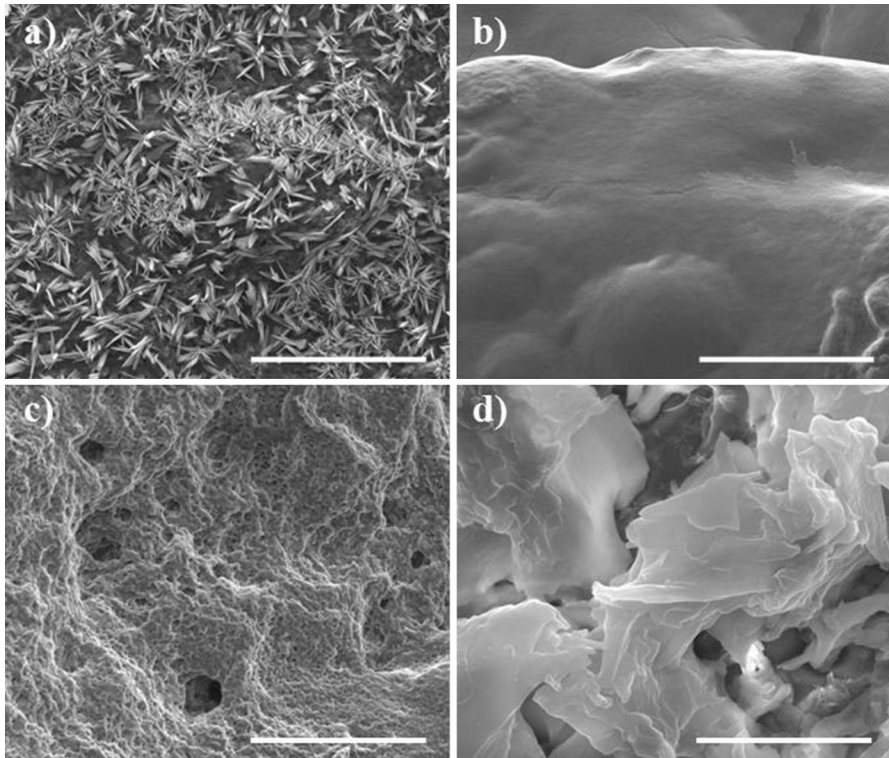
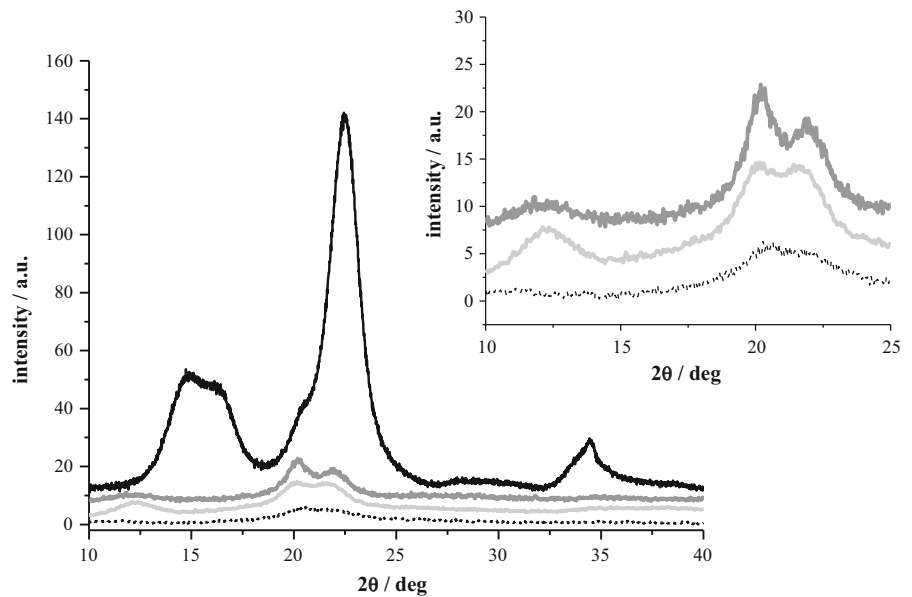


Fig. 5 SEM images of the cellulosic materials regenerated in acidic medium. Cellulose has been previously dissolved in a NaOH aqueous solution (*top left*), NaOH/urea aqueous solution

(*top right*), NaOH/thiourea aqueous solution (*bottom left*) or a TBAH aqueous solution (*bottom right*). The scale bar 10 μm

Fig. 6 X-ray diffraction patterns for native MCC (*full black curve*), and regenerated materials from MCC dissolved in an aqueous NaOH solvent (*dark grey curve*), in aqueous NaOH/thiourea solvent (*light grey curve*) and in the TBAH aqueous system (*dotted curve*). Inserted is the expanded interest region for regenerated samples. The insert highlights an expanded region of interest for the regenerated samples



addition of urea to the NaOH solvent can reduce the hydrophobic effect of cellulose since urea plays its role through interacting with the hydrophobic part of cellulose.

Other additives have also been investigated and in Table 2 the main chemical shifts for the solid and dissolved fractions of cellulose in 8 wt% NaOH based systems are summarized together with the type of crystalline arrangement of the undissolved cellulose (i.e. solid fraction).

The results indicate that the addition of selected additives to the NaOH solvent enhances the dissolution of cellulose (deduced by the increase of the intensity of the INEPT peaks and the decrease of the CP peaks intensity), in line with the PLM and SEM results; the amount of the solid fraction present in the solution not only decreases but the additive also affects the remaining crystalline organization.

Cellulose dissolution at extremely high pHs can be understood by the fact that cellulose molecules acquire net charges by deprotonation of the hydroxyl groups. The PTssNMR also provides strong evidence for changes in the protonation state of the hydroxyls since the chemical shifts change ca. 3 ppm when acidic solvents are used instead of basic ones (unpublished data). However, this will be further discussed in a subsequent paper about acid solvent systems. The higher solubility of cellulose at extreme pHs is based on the general finding that polyelectrolytes are more soluble in water than nonionic polymers, the driving force being the dissociation of counterions and the concomitant large counterion entropy. Additionally, most of the additives used here are suggested to reduce the hydrophobic interactions among cellulose chains.

The degree of dissolution, as well as the molecular arrangement of the solid fraction in solution, is expected to have an impact on the properties of the regenerated materials. In Fig. 5, SEM images of regenerated cellulose (precipitated in acidic medium) from the different alkali based aqueous systems are presented. After regeneration the material shows comparable features to the samples, which were observed by SEM without the acid medium coagulation. Similarly to what was previously observed in Fig. 2, the regenerated material from the NaOH aqueous solvent without any additive displays a highly crystalline structure. On the other hand, the solvents containing additives of intermediate polarity, such as urea or thiourea, lead to softer morphologies (no

needle-like crystals are observed) or even to a porous material, and clearly lacking in crystallinity. The decrease in crystallinity is evident from the X-ray analysis (Fig. 6).

The use of additives with amphiphilic properties such as urea, thiourea or APG in the NaOH system or using a solvent with an amphiphilic cation (TBAH) can be seen to considerably reduce the crystallinity of the native MCC. Regarding the position of the diffraction peaks, the starting MCC material presents a major sharp diffraction centered at ca. 22.5° (200) with a side peak at 20.5° (102) typical for a cellulose I crystalline organization. Other characteristic reflections from cellulose I type structure can be found at 14.7° (1–10), 16.6° (110) and 34.7° (004) (French 2014). When cellulose is dissolved in the NaOH aqueous solution or in the NaOH/thiourea system, and regenerated, the crystalline structure changes to a cellulose II type arrangement with two main diffraction peaks centered at 20.1° (110) and 21.9° (020), and a third reflection at 12.1° (1–10) (Nam et al. 2016). A more amorphous material with no detectable diffraction peaks is obtained when cellulose is regenerated from the TBAH aqueous system. The X-ray data are in good agreement with the NMR and SEM data.

Conclusions

A set of alkaline aqueous solvent systems for cellulose was used and significant differences both in the dissolved state and in the regenerated materials were identified. The combination of different characterization techniques demonstrates to be an excellent approach for obtaining reliable information about the molecular organization of cellulose in solution. PTssNMR is shown to be very powerful for the study of cellulose in solution and report on the solvent quality. The NaOH based solvent systems demonstrate to be more efficient in cellulose dissolution when additives of intermediate polarity are added. Significant changes in the CP and INEPT signals are observed for the systems containing NaOH and additives when compared with the NaOH aqueous system without additives. The solid fraction changes from a swelled state (NaOH aqueous) to cellulose II or an amorphous arrangement, in the presence of additives. Additionally, the peaks of the INEPT spectra are shifted in the presence of additives, possibly indicating a stronger

interaction between the less polar additives and the cellulose backbone. The use of an alkaline solvent with amphiphilic cations results in a marked enhancement of the dissolution rate and efficiency. This can be inferred from the poor CP signal obtained for the cellulose samples in aqueous TBAH and TBPH solutions. The regenerated materials present significant differences in morphology and crystallinity, depending on the solvent system used. The reduction in solvent polarity, obtained by addition of urea or thiourea, as well the use of TBAH, leads to smooth materials with lower degree of crystallinity. Overall the data highlight the amphiphilic properties of cellulose and the ability of a given solvent to weaken the hydrophobic interactions which consequently improves dissolution.

Acknowledgments This work was financially supported by the Crafoord foundation, Södra Skogsägarnas Stiftelse, Stiftelsen Nils och Dorthi Troëdssons forskningsfond, the Swedish Research Council (VR, Projects 2009-6794 and 2011-4334), and the Portuguese Foundation for Science and Technology (FCT, Projects PTDC/AGR-TEC/4049/2012 and PTDC/AGR-TEC/4814/2014, Researcher Grant IF/01005/2014 and PhD Grant SFRH/BD/80556/2011). The authors also acknowledge to ESMI (European Soft Matter Infrastructure) by the financial support (Proposal E141000607).

References

- Alves L, Medronho BF, Antunes FE, Romano A, Miguel MG, Lindman B (2015) On the role of hydrophobic interactions in cellulose dissolution and regeneration: colloidal aggregates and molecular solutions. *Colloids Surf A* 483:257–263. doi:10.1016/j.colsurfa.2015.03.011
- Bergensträhle-Wohlert M, Berglund L, Brady J, Larsson PT, Westlund P-O, Wohlert J (2012) Concentration enrichment of urea at cellulose surfaces: results from molecular dynamics simulations and NMR spectroscopy. *Cellulose* 19:1–12. doi:10.1007/s10570-011-9616-x
- Björklund S, Ruzgas T, Nowacka A, Dahi I, Topgaard D, Sparr E, Engblom J (2013) Skin membrane electrical impedance properties under the influence of a varying water gradient. *Biophys J* 104:2639–2650. doi:10.1016/j.bpj.2013.05.008
- French A (2014) Idealized powder diffraction patterns for cellulose polymorphs. *Cellulose* 21:885–896. doi:10.1007/s10570-013-0030-4
- Garvey CJ, Parker IH, Simon GP (2005) On the interpretation of X-ray diffraction powder patterns in terms of the nanostructure of cellulose I fibres. *Macromol Chem Phys* 206:1568–1575. doi:10.1002/macp.200500008
- Gustavsson S, Alves L, Lindman B, Topgaard D (2014) Polarization transfer solid-state NMR: a new method for studying cellulose dissolution. *RSC. Advances* 4:31836–31839. doi:10.1039/c4ra04415k
- Hao X et al (2015) Self-assembled nanostructured cellulose prepared by a dissolution and regeneration process using phosphoric acid as a solvent. *Carbohydr Polym* 123:297–304. doi:10.1016/j.carbpol.2015.01.055
- Hellstrand E, Nowacka A, Topgaard D, Linse S, Sparr E (2013) Membrane lipid co-aggregation with α -synuclein fibrils. *PLoS ONE* 8:e77235. doi:10.1371/journal.pone.0077235
- Ioelovich M (2012) Study of cellulose interaction with concentrated solutions of sulfuric acid. *ISRN. Chem Eng* 2012:7. doi:10.5402/2012/428974
- Kalashnikova I, Bizot H, Cathala B, Capron I (2012) Modulation of cellulose nanocrystals amphiphilic properties to stabilize oil/water interface. *Biomacromolecules* 13:267–275. doi:10.1021/bm201599j
- Kamida K, Okajima K, Matsui T, Kowsaka K (1984) Study on the solubility of cellulose in aqueous alkali solution by deuteration IR and ^{13}C NMR. *Polym J* 16:857–866. doi:10.1295/polymj.16.857
- Kamide K, Okajima K, Kowsaka K, Matsui T (1985) CP/MASS ^{13}C NMR spectra of cellulose solids: an explanation by the intramolecular hydrogen bond concept. *Polym J* 17:701–706. doi:10.1295/polymj.17.701
- Kihlman M, Medronho BF, Romano AL, Germgård U, Lindman B (2013) Cellulose dissolution in an alkali based solvent: influence of additives and pretreatments. *J Braz Chem Soc* 24:295–303
- Klemm D, Heublein B, Fink H-P, Bohn A (2005) Cellulose: fascinating biopolymer and sustainable raw material. *Angew Chem Int Ed* 44:3358–3393. doi:10.1002/anie.200460587
- Kunze J, Fink H-P (2005) Structural changes and activation of cellulose by caustic soda solution with urea. *Macromol Symp* 223:175–188. doi:10.1002/masy.200505012
- Langan P, Nishiyama Y, Chanzy H (2001) X-ray structure of mercerized cellulose II at 1 Å resolution. *Biomacromolecules* 2:410–416. doi:10.1021/bm005612q
- Lindman B, Karlström G, Stigsson L (2010) On the mechanism of dissolution of cellulose. *J Mol Liq* 156:76–81. doi:10.1016/j.molliq.2010.04.016
- Lu X, Shen X (2011) Solubility of bacteria cellulose in zinc chloride aqueous solutions. *Carbohydr Polym* 86:239–244. doi:10.1016/j.carbpol.2011.04.042
- Luo X, Zhang L (2013) New solvents and functional materials prepared from cellulose solutions in alkali/urea aqueous system. *Food Res Int* 52:387–400. doi:10.1016/j.foodres.2010.05.016
- Luo N, Lv Y, Wang D, Zhang J, Wu J, He J, Zhang J (2012) Direct visualization of solution morphology of cellulose in ionic liquids by conventional TEM at room temperature. *Chem Commun* 48:6283–6285. doi:10.1039/c2cc31483e
- Medronho B, Lindman B (2014) Competing forces during cellulose dissolution: from solvents to mechanisms. *Curr Opin Colloid Interface Sci* 19:32–40. doi:10.1016/j.cocis.2013.12.001
- Medronho B, Romano A, Miguel M, Stigsson L, Lindman B (2012) Rationalizing cellulose (in)solubility: reviewing basic physicochemical aspects and role of hydrophobic interactions. *Cellulose* 19:581–587. doi:10.1007/s10570-011-9644-6
- Mittal A, Katahira R, Himmel ME, Johnson DK (2011) Effects of alkaline or liquid-ammonia treatment on crystalline

- cellulose: changes in crystalline structure and effects on enzymatic digestibility. *Biotechnol Biofuels* 4:41. doi:[10.1186/1754-6834-4-41](https://doi.org/10.1186/1754-6834-4-41)
- Morris GA, Freeman R (1979) Enhancement of nuclear magnetic resonance signals by polarization transfer. *J Am Chem Soc* 101:760–762. doi:[10.1021/ja00497a058](https://doi.org/10.1021/ja00497a058)
- Nam S, French AD, Condon BD, Concha M (2016) Segal crystallinity index revisited by the simulation of X-ray diffraction patterns of cotton cellulose I β and cellulose II. *Carbohydr Polym* 135:1–9. doi:[10.1016/j.carbpol.2015.08.035](https://doi.org/10.1016/j.carbpol.2015.08.035)
- Nehls I, Wagenknecht W, Philipp B, Stscherbina D (1994) Characterization of cellulose and cellulose derivatives in solution by high resolution ^{13}C -NMR spectroscopy. *Prog Polym Sci* 19:29–78. doi:[10.1016/0079-6700\(94\)90037-X](https://doi.org/10.1016/0079-6700(94)90037-X)
- Nowacka A, Mohr PC, Norrman J, Martin RW, Topgaard D (2010) Polarization transfer solid-state NMR for studying surfactant phase behavior. *Langmuir* 26:16848–16856. doi:[10.1021/la102935t](https://doi.org/10.1021/la102935t)
- Nowacka A, Douezan S, Wadso L, Topgaard D, Sparr E (2012) Small polar molecules like glycerol and urea can preserve the fluidity of lipid bilayers under dry conditions. *Soft Matter* 8:1482–1491. doi:[10.1039/c1sm06273e](https://doi.org/10.1039/c1sm06273e)
- Nowacka A, Bongartz NA, Ollila OHS, Nylander T, Topgaard D (2013) Signal intensities in ^1H – ^{13}C CP and INEPT MAS NMR of liquid crystals. *J Magn Reson* 230:165–175. doi:[10.1016/j.jmr.2013.02.016](https://doi.org/10.1016/j.jmr.2013.02.016)
- O'Connor RT, DuPré EF, Mitcham D (1958) Applications of infrared absorption spectroscopy to investigations of cotton and modified cottons: part I: physical and crystalline modifications and oxidation. *Text Res J* 28:382–392. doi:[10.1177/004051755802800503](https://doi.org/10.1177/004051755802800503)
- Pines A, Gibby MG, Waugh JS (1972) Proton-enhanced nuclear induction spectroscopy. A method for high resolution NMR of dilute spins in solids. *J Chem Phys* 56:1776–1777. doi:[10.1063/1.1677439](https://doi.org/10.1063/1.1677439)
- Porro F, Bédué O, Chanzy H, Heux L (2007) Solid-state ^{13}C NMR study of Na-cellulose complexes. *Biomacromolecules* 8:2586–2593. doi:[10.1021/bm0702657](https://doi.org/10.1021/bm0702657)
- Rein DM, Khalfin R, Szekely N, Cohen Y (2014) True molecular solutions of natural cellulose in the binary ionic liquid-containing solvent mixtures. *Carbohydr Polym* 112:125–133. doi:[10.1016/j.carbpol.2014.05.059](https://doi.org/10.1016/j.carbpol.2014.05.059)
- Sen S, Martin JD, Argyropoulos DS (2013) Review of cellulose non-derivatizing solvent interactions with emphasis on activity in inorganic molten salt hydrates. *ACS Sustain Chem Eng* 1:858–870. doi:[10.1021/sc400085a](https://doi.org/10.1021/sc400085a)
- Široký J, Blackburn R, Bechtold T, Taylor J, White P (2010) Attenuated total reflectance Fourier-transform Infrared spectroscopy analysis of crystallinity changes in lyocell following continuous treatment with sodium hydroxide. *Cellulose* 17:103–115. doi:[10.1007/s10570-009-9378-x](https://doi.org/10.1007/s10570-009-9378-x)
- Takai M, Colvin JR (1978) Mechanism of transition between cellulose I and cellulose II during mercerization. *J Polym Sci Polym Chem Ed* 16:1335–1342. doi:[10.1002/pol.1978.170160614](https://doi.org/10.1002/pol.1978.170160614)
- VanderHart DL, Atalla RH (1984) Studies of microstructure in native celluloses using solid-state carbon-13 NMR. *Macromolecules* 17:1465–1472. doi:[10.1021/ma00138a009](https://doi.org/10.1021/ma00138a009)
- Wernersson E, Stenqvist B, Lund M (2015) The mechanism of cellulose solubilization by urea studied by molecular simulation. *Cellulose*. doi:[10.1007/s10570-015-0548-8](https://doi.org/10.1007/s10570-015-0548-8)
- Xiong B, Zhao P, Hu K, Zhang L, Cheng G (2014) Dissolution of cellulose in aqueous NaOH/urea solution: role of urea. *Cellulose* 21:1183–1192. doi:[10.1007/s10570-014-0221-7](https://doi.org/10.1007/s10570-014-0221-7)
- Yamane C, Aoyagi T, Ago M, Sato K, Okajima K, Takahashi T (2006) Two different surface properties of regenerated cellulose due to structural anisotropy. *Polym J* 38:819–826
- Yan L, Gao Z (2008) Dissolving of cellulose in PEG/NaOH aqueous solution. *Cellulose* 15:789–796. doi:[10.1007/s10570-008-9233-5](https://doi.org/10.1007/s10570-008-9233-5)
- Zhang S, Wang W-C, Li F-X, Yu J-Y (2013) Swelling and dissolution of cellulose in NaOH aqueous solvent systems. *Cellul Chem Technol* 47:671–679
- Zumbulyadis N (1983) Selective carbon excitation and the detection of spatial heterogeneity in cross-polarization magic-angle-spinning NMR. *J Magn Reson* 53:486–494. doi:[10.1016/0022-2364\(83\)90219-6](https://doi.org/10.1016/0022-2364(83)90219-6)